**Dynamic Modeling and Control Design**

**of a**

# ROBOTIC BACKHOE WITH HAPTIC DISPLAY

Joe Frankel

Georgia Institute of Technology

April 24, 2003

## I. Introduction

### *A. Background*

The traditional method to control hydraulic equipment has been accomplished with the use of manual proportional valves. For example, a typical diesel powered earthmoving vehicle generates hydraulic pressure with a pump, which is mechanically driven by the engine. The pump delivers hydraulic power to its implements, such as a backhoe, loader, or auger, via manual valves that are controlled by the operator. A direct mechanical connection exists between the operator's hand and the spool in the valve through a lever and connecting linkages. The spool must be displaced from its zero position to allow high-pressure fluid to flow from the pump to the cylinders and cause the implement to move. Each lever may control either one or two degrees of freedom of the implement.

A backhoe operator must control multiple levers simultaneously in order to produce the desired end-effector (bucket) motion, which is a skill that takes time to learn. Also, feedback information on the forces experienced by the bucket is limited, in the form of compliance in the levers due to cylinder pressure changes, engine speed changes under load, and vehicle vibration.

The purpose of this project is to explore the viability of applying modern control techniques to hydraulic earthmoving equipment. The current design includes state feedback control and haptic force display to the operator's hand. It is proposed that with proper control system design, the implement's performance and user interface can both be improved for greater productivity and shorter operator training time, without significant increases in manufacturing costs.

### *B. The Robotic Backhoe with Haptic Display*

Figure 1 illustrates the system under investigation. The John Deere Model 47 backhoe attachment is mounted on a 4410 tractor. The master manipulator is the Personnel Haptic Interface Mechanism (PHANTOM), hereafter referred to as the master, developed at MIT and produced commercially by Sensable Technologies. Additional proposed components include solenoid valves, angle encoders, and a PC-104 controller.

Figure 1: Robotic Backhoe with Haptic Display

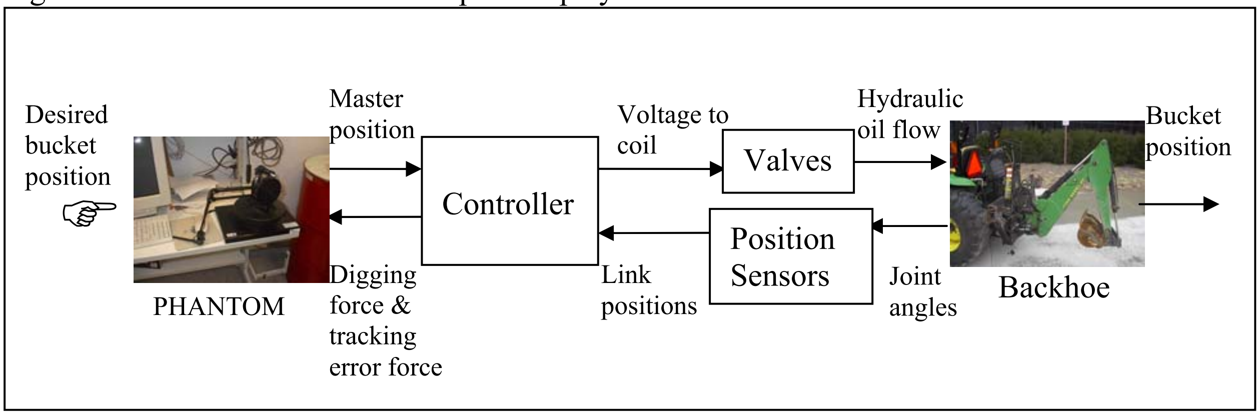


Figure 1 is a block diagram of the system under consideration. The desired bucket position is defined as the input and the actual bucket position as the output. Several simplifications and assumptions will be made to the system shown in Figure 1. A dynamic state space model will be derived, a potential controller will be proposed, and simulation results will be presented.

## II. Component Modeling

### *A. Valve and Cylinder*

Figure 2 illustrates an electrically actuated proportional valve connected to a hydraulic cylinder.

Figure 2: Valve and Cylinder

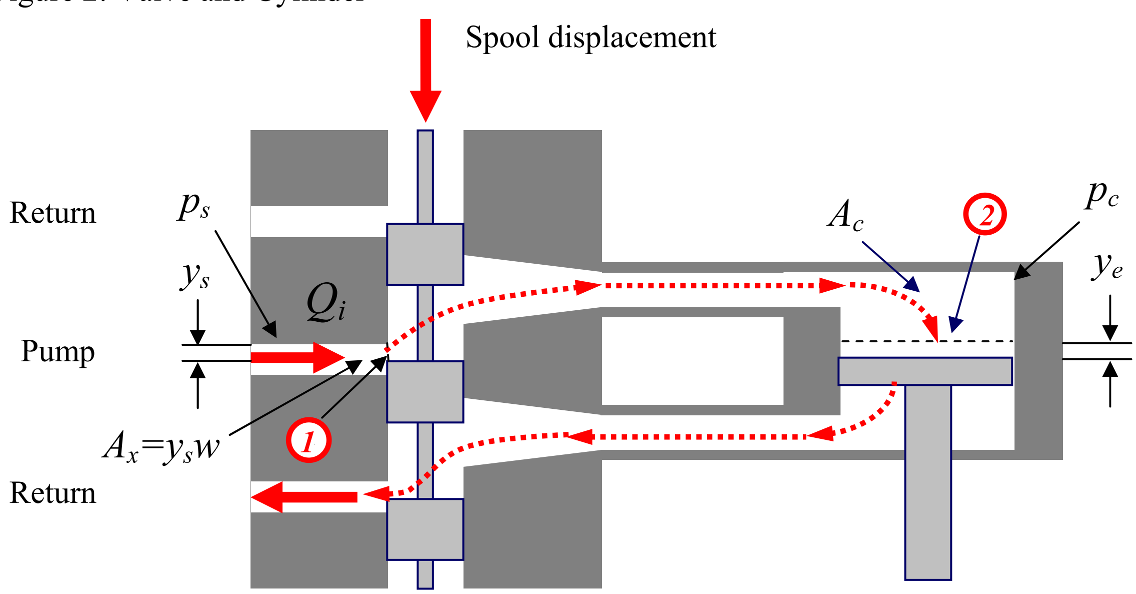

When the valve spool is displaced from $y_s=0$, a series of events occur, which can be described by the following equations. Assuming incompressible fluid and conservation of mass, the flow through the valve into the cylinder is

$$A_x V_x = A_c V_c = Q_i \tag{1}$$

where $A_x$ denotes the cross section of the opening between the spool and valve body, $A_x=y_s w$ and $w$ is the spool's width. $A_c$ is the cylinder area, $V_x$ and $V_c$ are the fluid velocities, and $Q_i$ is the flow rate.

Assuming inviscid fluid and no energy losses between points 1 and 2, conservation of energy along a streamline requires that

$$p_s + \frac{1}{2}\rho V_x^{\,2} = p_c + \frac{1}{2}\rho V_c^{\,2} \tag{2}$$

where $p_s$ and $p_c$ are the supply pressure and cylinder pressure, and $\rho$ is the fluid density. Combining equations (1) and (2) and solving for the flow rate results in

$$Q_i = \sqrt{\frac{2A_c^{\,2}(p_s - p_c)}{1 - \frac{A_c^{\,2}}{(y_s w)^2}}} = f(y_s, p_c) \tag{3}$$

which shows that the flow rate into the cylinder is a function of spool displacement and cylinder pressure, assuming constant supply pressure from the pump. Equation (3) can be linearized about operating points $\bar{y}_s$ and $\bar{p}_c$,

$$Q_i \cong \left.\frac{\partial Q_i}{\partial y_s}\right|_{\bar{y}_s, \bar{p}_c} (y_s - \bar{y}_s) + \left.\frac{\partial Q_c}{\partial p_c}\right|_{\bar{y}_s, \bar{p}_c} (p_c - \bar{p}_c) = k_y \hat{y}_s + k_p \hat{p}_c \tag{4}$$

where the sensitivity of fluid flow with respect to cylinder pressure $k_p$ is negative and $\hat{p}_c$ is the differential pressure across the cylinder because the equilibrium pressures are equal.

Neglecting the dynamics of the valve spool, the spool position is assumed to be proportional to the driving voltage sent to the coil:

$$\hat{y}_s = K_{coil} \hat{V}_{coil} \tag{5}$$

### *B. Rod, Bucket and Soil*

Neglecting the kinematics of the backhoe's links, the rod and bucket will be modeled as a single rigid mass, as illustrated in Figure 3.
Figure 3: Rod and Bucket

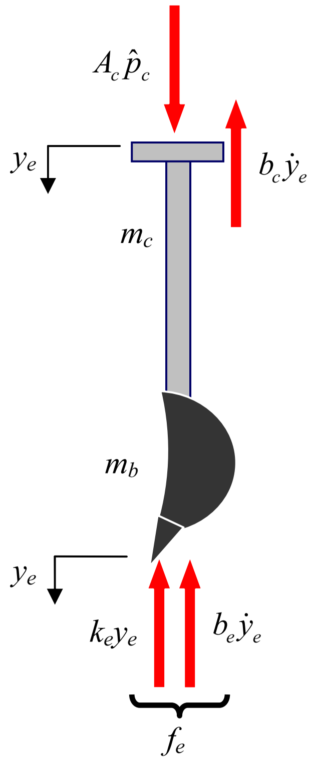


Applying Newton's second law on the rod/bucket mass, equation (6) describes the motion of the bucket:

$$A_c\hat{p}_c - b_c\dot{y}_e - f_e = (m_c + m_b)\ddot{y}_e \tag{6}$$

where the cross-sectional area of the rod has been neglected and $\hat{p}_c$ is the net hydraulic pressure acting on the cylinder.

The soil is modeled as a passive compliance:

$$f_e = b_e\dot{y}_e + k_e y_e \tag{7}$$

Note that the values of be and ke will vary dramatically, depending on the soil's composition, density, moisture content, etc. For this simulation, the values of $b_e$=*2x10*$^7$ *Ns/m* and $k_e$=*5x10*$^3$ *N/m* have been used.

### *C. Bucket Dynamics*

Substituting equations (1) and (5) into (4) gives

$$A_c \dot{y}_e = k_y K_{coil} \hat{V}_{coil} + k_p \hat{p}_c \tag{8}$$

where $\dot{y}_e = V_c$. Solving (8) for the differential cylinder pressure,

$$\hat{p}_c = \frac{A_c}{k_p}\dot{y}_e - \frac{k_y K_{coil}}{k_p}\hat{V}_{coil} \tag{9}$$

Substituting equations (9) and (7) into (6),

$$A_c\left[\frac{A_c}{k_p}\dot{y}_e - \frac{k_y K_{coil}}{k_p}\hat{V}_{coil}\right] - b_c\dot{y}_e - \left[b_e\dot{y}_e + k_e y\right] = \left(m_c + m_b\right)\ddot{y}_e \tag{10}$$

and then rearranging (10) results in the dynamic equation of the bucket motion in terms of the voltage input to the coil in the valve:

$$\ddot{y}_e = \left[\frac{{A_c}^2 / k_p - \left(b_e + b_c\right)}{m_c + m_b}\right]\dot{y}_e - \left[\frac{k_e}{m_c + m_b}\right]y_e - \left[\frac{A_c k_y K_{coil}}{\left(m_c + m_b\right)k_p}\right]\hat{V}_{coil} \tag{11}$$

or more simply

$$\ddot{y}_e = a_1\dot{y}_e + a_2 y_e + b_1\hat{V}_{coil} \tag{12}$$

The coefficients in (12) can be found in (11) by inspection.

### *D. The Human Operator*

The human operator will be modeled as if providing proportional error feedback, where the force exerted on the master is proportional to the error between the desired and actual bucket location:

$$F_{hand} = K_{user}(y_{des} - y_e) \tag{13}$$

### *E. Haptic Display forces*

Two forces are represented and displayed haptically to the user's hand by the master. The first force is the digging force, which is proportional to the differential cylinder pressure:

$$F_{for} = K_{for}\hat{p}_c \tag{14}$$

The second force is the tracking error force, which is proportional to the tracking error between the master position and bucket position, scaled by the workspace scaling ratio:

$$F_{pos} = K_{pos}\left(K_{scale}y_m - y_e\right) \tag{15}$$

where $y_m$ is the master position and $K_{scale}$ is the ratio of the bucket workspace to the master workspace.

### *F. Phantom Dynamics*

Figure 4 shows the forces acting on the master. The input force $F_{hand}$ is supplied by the operator, and $F_{for}$ and $F_{pos}$ are calculated by the controller and represented by the actuators in the master. The damping force $b_m\dot{y}_m$ resisting the master velocity has been added to improve stability.

Figure 4: Forces on the master

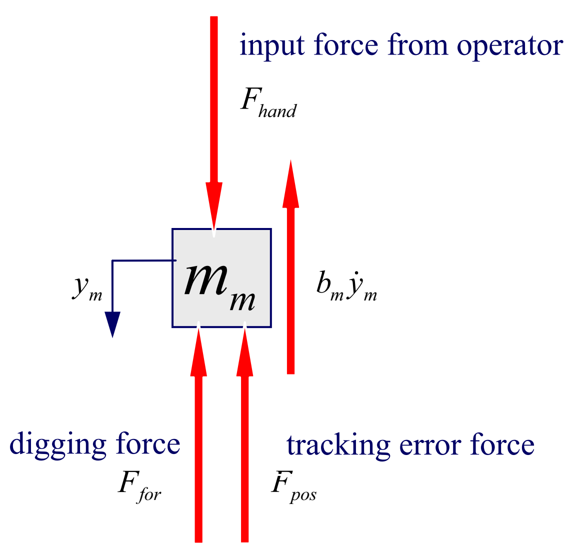


Applying Newton's 2nd Law to the master yields

$$F_{hand} - F_{for} - F_{pos} - b_m\dot{y}_m = m_m\ddot{y}_m \tag{16}$$

Substituting equations (13), (14), and (15) into (16) yields

$$K_{user}(y_{des} - y_e) - K_{for}\hat{p}_c - K_{pos}(K_{scale}y_m - y_e) - b_m\dot{y}_m = m_m\ddot{y}_m \tag{17}$$

Substituting equation (9) into (17) and solving for the master acceleration $\ddot{y}_m$ yields the equation of motion of the master in terms of the desired bucket position $y_{des}$ and the voltage to the valve coil $\hat{V}_{coil}$:

$$\ddot{y}_m = -\frac{b_m}{m_m}\dot{y}_m - \frac{K_{pos}K_{scale}}{m_m}y_m - \frac{K_{for}A_c}{m_m k_p}\dot{y}_e + \frac{(K_{pos} - K_{user})}{m_m}y_e + \frac{K_{for}k_y K_{coil}}{m_m k_p}\hat{V}_{coil} + \frac{K_{user}}{m_m}y_{des} \tag{18}$$

or more simply,

$$\ddot{y}_m = a_3\dot{y}_m + a_4 y_m + a_5\dot{y}_e + a_6 y_e + b_2\hat{V}_{coil} + b_3 y_{des} \tag{19}$$

and the coefficients in (19) can be found in (18) by inspection. Note that this is a two-input system, $y_{des}$ from the operator and $\hat{V}_{coil}$ from the yet-to-be-determined controller, and the master's dynamics are coupled with the bucket's dynamics via the haptic display forces.

## III. System Modeling

### *A. Open-Loop State Space Model*

Defining the state variables

$$x_1 = y_e,\ x_2 = y_m,\ x_3 = \dot{y}_e,\ x_4 = \dot{y}_m \tag{20}$$

and using equations (12) and (19), the continuous time state space equations for the open-loop plant are

$$\begin{bmatrix} \dot{x}_1(t) \\ \dot{x}_2(t) \\ \dot{x}_3(t) \\ \dot{x}_4(t) \end{bmatrix} = \begin{bmatrix} 0 & 0 & 1 & 0 \\ 0 & 0 & 0 & 1 \\ a_2 & 0 & a_1 & 0 \\ a_6 & a_4 & a_5 & a_3 \end{bmatrix} \begin{bmatrix} x_1(t) \\ x_2(t) \\ x_3(t) \\ x_4(t) \end{bmatrix} + \begin{bmatrix} 0 & 0 \\ 0 & 0 \\ b_1 & 0 \\ b_2 & b_3 \end{bmatrix} \begin{bmatrix} \hat{V}_{coil}(t) \\ y_{des}(t) \end{bmatrix}$$

$$y_e = \begin{bmatrix} 1 & 0 & 0 & 0 \end{bmatrix} \begin{bmatrix} x_1(t) \\ x_2(t) \\ x_3(t) \\ x_4(t) \end{bmatrix} \tag{21}$$

or

$$\dot{x}(t) = Ax(t) + Bu(t)$$
$$y_e(t) = Cx(t) \tag{22}$$

### *B. Discretization*

The discrete time state matrices *G* and *H* corresponding to the continuous time state matrices are found by solving the convolution integral over one time step *T*:

$$x((k+1)T) = e^{AT}x(kT) + \int_0^T e^{At}Bdt\,u(kT) \tag{23}$$

where

$$G = e^{At}\Big|_{t=T}, \quad H = \int_0^T e^{At}Bdt \tag{24}$$

and the input is assumed constant over the interval. For a linear time-invariant system, the state transition matrix $\Psi(t) = e^{At}$ can be found either with the Laplace Transform method,

$$e^{At} = L^{-1}\left[(sI - A)^{-1}\right] \tag{25}$$

or a Taylor Series expansion

$$e^{At} = \sum_{n=0}^{\infty} \frac{d^n\left(e^{At}\right)}{dt^n}\frac{1}{n!} = I + At + \frac{A^2t^2}{2!} + \cdots \tag{26}$$

resulting in the discrete state matrix equation

$$x(k+1) = Gx(k) + Hu(k) \tag{27}$$

where the time step *T* is implicit and has been removed for clarity. In this report, the Matlab function `'c2d'` has been used to compute the values of *G* and *H*.

### *C. Velocity Observer*

It is assumed that the master and bucket will both possess position sensors allowing for direct feedback control on $y_e$ and $y_m$. It is also assumed that neither of the velocities $\dot{y}_e$ and $\dot{y}_m$ will be available; therefore, an observer will be required to provide feedback on these states.

Partitioning equation (21) into measurable and immeasurable states and defining the output as the measurable states, the open-loop plant becomes

$$\begin{bmatrix} x_a(k+1) \\ x_b(k+1) \end{bmatrix} = \begin{bmatrix} G_{aa} & G_{ab} \\ G_{ba} & G_{bb} \end{bmatrix} \begin{bmatrix} x_a(k) \\ x_b(k) \end{bmatrix} + \begin{bmatrix} H_{a1} & H_{a2} \\ H_{b1} & H_{b2} \end{bmatrix} \begin{bmatrix} \hat{V}_{coil}(k) \\ y_{des} \end{bmatrix}$$
$$y(k) = [I \quad 0] \begin{bmatrix} x_a(k) \\ x_b(k) \end{bmatrix} = x_a(k) \tag{28}$$

where the measurable states are $x_a(k) = \begin{bmatrix} y_e & y_m \end{bmatrix}^T$ and the immeasurable states are $x_b(k) = \begin{bmatrix} \dot{y}_e & \dot{y}_m \end{bmatrix}^T$. The system to be observed is

$$x_b(k+1) = G_{bb} x_b(k) + G_{ba} y(k) + H_{b1} \hat{V}_{coil}(k) + H_{b2} y_{des}(k) \tag{29}$$

Rearranging the first submatrix equation in (28) results in

$$x_a(k+1) - G_{aa} x_a(k) - H_{a1} \hat{V}_{coil}(k) - H_{a2} y_d(k) = G_{ab} x_b(k) \tag{30}$$

The velocity state observer is defined as:

$$\hat{x}_b(k+1) = G_{bb} \hat{x}_b(k) + G_{ba} y(k) + H_{b1} \hat{V}_{coil}(k) + H_{b2} y_{des}(k) + \left[ L G_{ab} \left( x_b(k) - \hat{x}_b(k) \right) \right] \tag{31}$$

where $\hat{x}_b(k)$ is a replica of the immeasurable states and the last term on the right corrects for observer inaccuracies. Substituting equation (30) into (31), replacing $x_a(k+1)$ with $y(k+1)$ and rearranging gives

$$\begin{aligned} \hat{x}_b(k+1) = \left( G_{bb} - L G_{ab} \right) \hat{x}_b(k) + \left( H_{b1} - L H_{a1} \right) \hat{V}_{coil}(k) + \left( H_{b2} - L H_{a2} \right) y_{des}(k) \\ + \left( G_{ba} - L G_{aa} \right) y(k) + L y(k+1) \end{aligned} \tag{32}$$

Equation (32) cannot be directly augmented into the state matrix because of the term $y(k+1)$ on the right hand side. To alleviate this problem, define

$$\eta(k) = \hat{x}_b(k) - L y(k) \tag{33}$$

then

$$\begin{aligned} \eta(k+1) &= \hat{x}_b(k+1) - L y(k+1) \\ &= \left( G_{bb} - L G_{ab} \right) \hat{x}_b(k) + \left( H_{b1} - L H_{a1} \right) \hat{V}_{coil}(k) + \left( H_{b2} - L H_{a2} \right) y_{des}(k) + \left( G_{ba} - L G_{aa} \right) y(k) \end{aligned} \tag{34}$$

and rearranging

$$\eta(k+1) = (G_{bb} - LG_{ab})\eta(k) + (G_{bb}L - LG_{ab}L + G_{ba} - LG_{aa})y(k) + (H_{b1} - LH_{a1})\hat{V}_{coil}(k) + (H_{b2} - LH_{a2})y_{des}(k) \tag{35}$$

and

$$\hat{x}_b(k) = \eta(k) + Lx_a(k) \tag{36}$$

where *y(k)* was replaced with $x_a(k)$ in (30). This will be used later for feedback on the immeasurable velocity states. In the simulations that follow, the observer gains *L* were chosen such that the observer exhibited deadbeat response, i.e. the poles of $G_{bb}$-$LG_{ab}$ were placed at the origin in the z-plane.

### *D. Integrated Error*

Define a new state that sums all of the errors between the scaled master position and bucket position from the starting point to the previous time step:

$$\sigma(k) = \sum_{i=1}^{k-1}\left(K_{scale}y_m(i) - y_e(i)\right) \tag{37}$$

then the next value of *σ(k)* will be

$$\sigma(k+1) = K_{scale}y_m(k) - y_e(k) + \sigma(k) \tag{38}$$

Defining an error vector,

$$E = \begin{bmatrix} -1 & K_{scale} \end{bmatrix} \tag{39}$$

equation (38) becomes

$$\sigma(k+1) = E\begin{bmatrix} y_e(k) \\ y_m(k) \end{bmatrix} + \sigma(k) = Ex_a(k) + \sigma(k) \tag{40}$$

### *E. Augmented State Equation*

Combining equations (28), (35), and (40) results in the augmented state equation, now increased in order by three from the observer and integration equations, to a total of seven states:

$$\begin{bmatrix} x_a(k+1) \\ x_b(k+1) \\ \eta(k+1) \\ \sigma(k+1) \\ \end{bmatrix} = \begin{bmatrix} G_{aa} & G_{ab} & 0 & 0 \\ G_{ba} & G_{bb} & 0 & 0 \\ H_y & 0 & G_r & 0 \\ E & 0 & 0 & 1 \end{bmatrix} \begin{bmatrix} x_a(k) \\ x_b(k) \\ \eta(k) \\ \sigma(k) \\ \end{bmatrix} + \begin{bmatrix} H_{a1} \\ H_{b1} \\ H_{u1} \\ 0 \end{bmatrix} \hat{V}_{coil}(k) + \begin{bmatrix} H_{b1} \\ H_{b2} \\ H_{u2} \\ 0 \end{bmatrix} y_{des}$$

$$y_e(k) = [1 \quad 0 \quad 0 \quad 0 \quad 0 \quad 0 \quad 0] \begin{bmatrix} x_a(k) \\ x_b(k) \\ \eta(k) \\ \sigma(k) \\ \end{bmatrix} \tag{41}$$

where $H_y = (G_{bb}L - LG_{ab}L + G_{ba} - LG_{aa})$, $G_r = (G_{bb} - LG_{ab})$, $H_{u1} = (H_{b1} - LH_{a1})$, and $H_{u2} = (H_{b2} - LH_{a2})$ from (35). Thus the immeasurable states are available via the observer *η(k)* in equation (41), via equation (36), and the integrated sum of the errors are available as *σ(k)*.

## IV. Controller Design

Equation (41) can be written more compactly as

$$x(k+1) = G_o x(k) + H_1 \hat{V}_{coil}(k) + Hy_{des}(k) \tag{42}$$

The final step that remains is to relate the input to the plant $\hat{V}_{coil}$ to the other state variables. Define the control law as

$$\hat{V}_{coil}(k) = K_p\left(K_{scale} y_m(k) - y_e(k)\right) + K_v(K_{scale}\dot{\hat{y}}_m(k) - \dot{\hat{y}}_e(k)) + K_I \sum_{i=1}^{k-1}\left(K_{scale} y_m(i) - y_e(i)\right) \tag{43}$$

which is a form of a PID controller. Substituting equation (39) into (43) and using the partitioned states yields

$$\hat{V}_{coil}(k) = K_p E x_a(k) + K_v E \hat{x}_b(k) + K_I \sigma(k) \tag{44}$$

and substituting equation (36) into (44) and rearranging gives

$$\hat{V}_{coil}(k) = \begin{bmatrix} K_p E + K_v EL & 0 & K_v E & K_I \end{bmatrix} \begin{bmatrix} x_a(k) \\ x_b(k) \\ \eta(k) \\ \sigma(k) \\ \end{bmatrix} = K_c x(k) \tag{45}$$

Finally, substituting (45) into (41) yields the final form of the state equation, including velocity observer, full state feedback, and PID control:

$$x(k+1) = \left(G_o + H_1 K_c\right)x(k) + H y_{des}(k)$$
$$y_e(k) = \begin{bmatrix} C & 0 & 0 & 0 \end{bmatrix} x(k) \qquad (46)$$

## V. Simulation

### *A. Parameter and Gain Selection*

The system derived above was coded into Matlab using the system parameters and gains listed in Table 1.

Table 1: System Parameters and Control Gains

| ***Variable*** | ***Description*** | ***Value*** | ***Units*** |
|---|---|---|---|
| **System Parameters** | | | |
| $A_c$ | Cylinder area | 0.08 | $m^2$ |
| $m_c$ | Rod mass | 50 | kg |
| $m_b$ | Bucket mass | 50 | kg |
| $k_y$ | Valve sensitivity to spool position | 5 | $m^2/s$ |
| $k_p$ | Valve sensitivity to pressure changes | $-4 \cdot 10^{-9}$ | $m^3/Pa \cdot s$ |
| $K_{coil}$ | Spool position/voltage gain | 0.004 | m/V |
| $b_c$ | Cylinder friction | 0.1 | N·s/m |
| $b_e$ | Soil damping coefficient | $2 \cdot 10^{-7}$ | N·s/m |
| $k_e$ | Soil spring coefficient | $5 \cdot 10^{-3}$ | N/m |
| $m_m$ | Mass of master | 0.05 | kg |
| | | | |
| **Control Gains** | | | |
| $K_{scale}$ | Workspace scaling ratio | 12 | m/m |
| $b_m$ | Master damping coefficient | 5 | N·s/m |
| $K_{user}$ | Operator force/error gain | 1 | N/m |
| $K_{pos}$ | Haptic tracking error gain | 20 | N/m |
| $K_{for}$ | Haptic digging force gain | $6 \cdot 10^{-9}$ | N/Pa |
| $K_p$ | Proportional state feedback gain | 30 | V/m |
| $K_v$ | Velocity state feedback gain | 4 | V·s/m |
| $K_I$ | Integral state feedback gain | 60 | V/ m·s |

These values may be found in the Matlab code given at the end of the report.

*B. Step Response*

Using the values listed in Table 1, the system response to a step input $y_{des}=1m$ is illustrated in Figure 5.

Figure 5: System Step Response

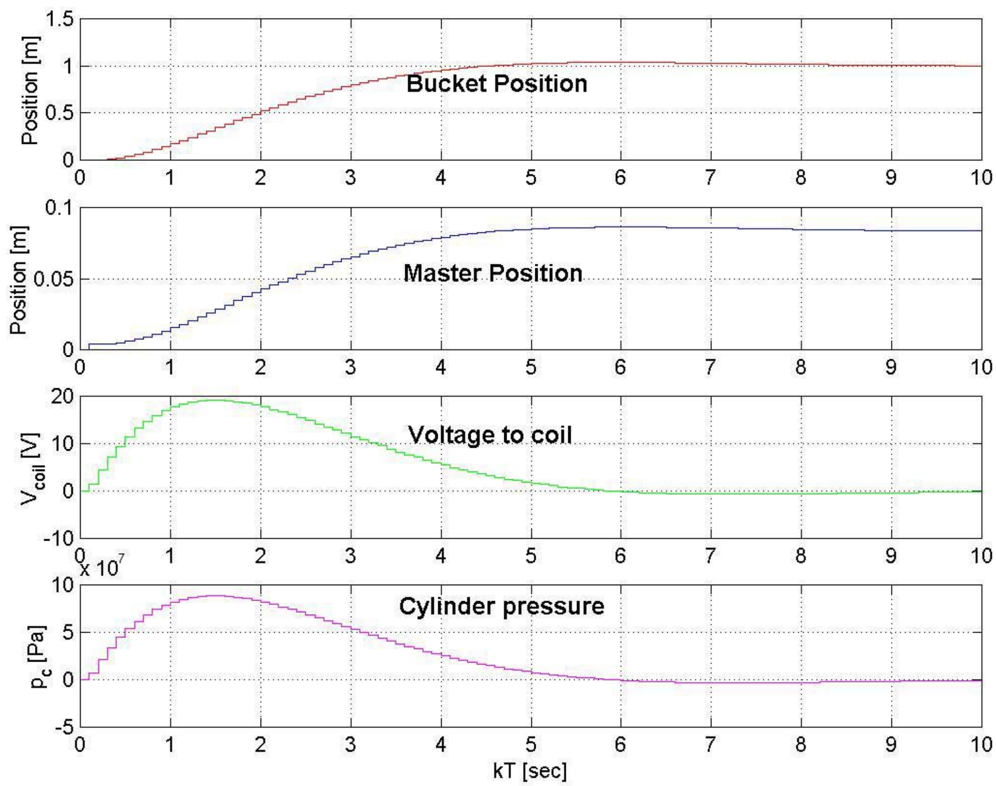


Figure 5 illustrates the positions of the bucket and master, as well as the driving voltage sent to the valve coil (control effort) and the estimated cylinder pressure in response to a step input. Physically, this would represent the bucket being forced one meter downward into the soil, starting at ground level $y_e$=0. Note that the system reaches steady state in approximately five seconds and exhibits no steady state error. Also, note that the final position of the master is the same as the scaled position of the bucket, where $K_{scale}y_m=(12)(0.083m)=1m=y_e$. The cylinder pressure is computed from equation (9), where the estimated cylinder velocity has been used from the observer,

$$\dot{\hat{y}}_e(k) = \eta_1(k) + L_{1,1}y_e(k) + L_{1,2}y_m(k)\,.$$

Figure 6 illustrates the position error and integrated error during the simulation. The error is defined as the difference between the bucket position and the scaled master position, $error=K_{scale}y_m-y_e$.

Figure 6: System Error

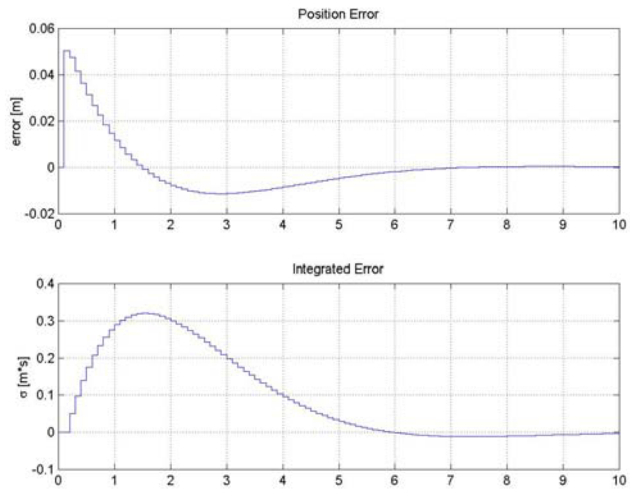


Figure 6 illustrates that the simulated system exhibits zero steady state error due to the combination of feedback on the two error signals.

### *C. System Robustness to Parameter Variations*

In practice, it is expected that the system parameters most likely to vary will be the soil properties. Figure 7 illustrates the step response of the system after a *decrease by a factor of ten* in the spring and damping coefficients of the soil.

Figure 7: System Step Response after soil property change.

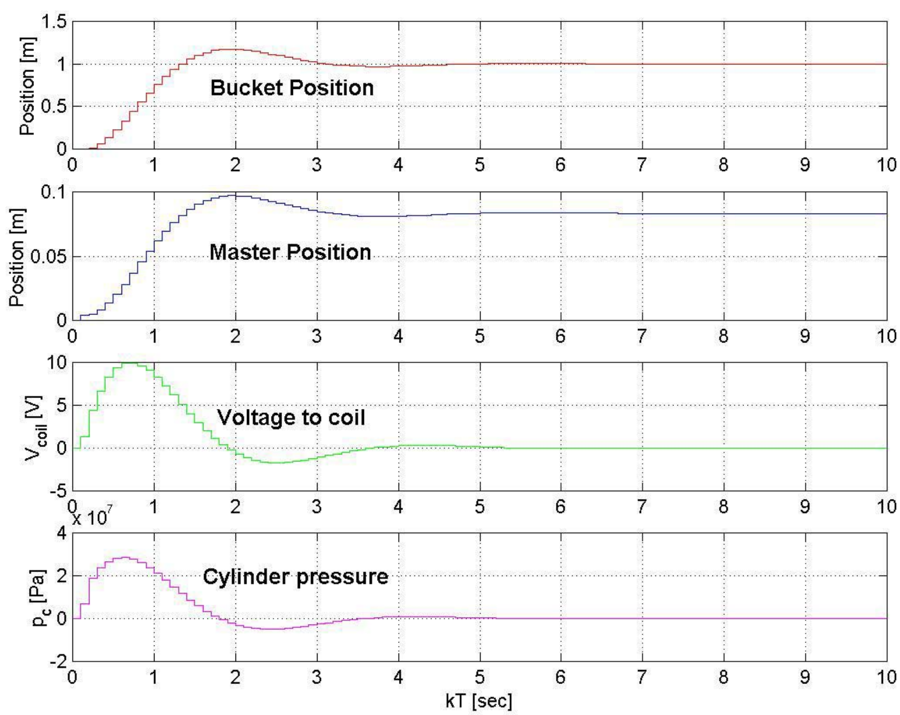


Thus the simulated system is robust to changes in soil properties.

## VI. Conclusions

A simplified dynamic model of the Robotic Backhoe with Haptic Display has been derived, a PID controller has been designed, and simulations presented. At this time, although the results are inconclusive as to whether a backhoe's performance can be improved, they are promising.

Currently, many of the system components have yet to be specified. Therefore, the system parameters listed in Table 1 had to be chosen judiciously from catalogs, manuals, and rough measurements on the backhoe. In the end, most of the values used were estimations, and gains were then chosen to produce a desirable response. The system parameters will need to be updated and the gains adjusted once the valves, sensors, and other equipment becomes available.

For several reasons, it is suspected that the greatest contributor to modeling inaccuracies will be in the valve. First, since the flow equation has been linearized about a nominal operating point, any significant deviation from this point will contribute to error.

Second, it is expected that the valve will be in saturation—i.e. at maximum flow and at the end of the spool's travel—during much of its operation. This factor has been accounted for in equation (4) by increasing the flow sensitivity to $k_y=5m^2/s$, a value that is overestimated based upon the flow rates given for typical proportional valves in this GPM range.

Third, most lower-end proportional valves have a deadband such that the valve exhibits zero flow over a range around zero, and consequently cannot reverse flow instantaneously.

Finally, the response time of many proportional valves is on the order of 50 ms, so the backhoe's speed will be limited by this factor in addition to the maximum flow rate.

Soil properties are expected to vary depending on composition, density, moisture content, etc. In addition, the passive compliance model given in equation (7) will vary depending on the geometry of the bucket.

The next step is to extend the model to include 3-D link space kinematics, simulate the system dynamics by computing the geometric Jacobian, and solving the forward dynamics equations at every time step. Much of this work has been performed, and only needs to be incorporated with the control design contained herein. The result of this extended model will certainly be an important milestone in the development of the Robotic Backhoe with Haptic Display.

## VII. Matlab Code

```
% BACKHOE 1-D POSITION CONTROL w/HAPTIC FORCE FEEDBACK

close all ; clear all ; clc ;

% Joystick parameters
mm=0.05;
bm=5;
Kfor=6e-9;
Kpos=20;
Kscale=12;
Kuser=1;

% PID Controller Parameters
T=0.1;
KP=30;
KV=4;
KI=60;

% Valve parameters
Kcoil=0.004;
ky=5;
kp=-4e-9;

% Cylinder parameters
Ac=0.08;                              % ~4" dia cylinder
bc=0.1;
mc=50;

% Bucket parameters
mb=50;

% Soil parameters
ke=5e3
be=2e7;

% Simulation time vector
t=0:T:1e2*T;

% Define constants/coefficients
a1=(Ac^2/kp-(bc+be))/(mc+mb);
a2=-ke/(mc+mb);
b1=(-Ac*ky*Kcoil)/((mc+mb)*kp);

a3=-bm/mm;
a4=-Kpos*Kscale/mm;
a5=-(Kfor*Ac)/(mm*kp);
a6=(Kpos-Kuser)/mm;
b2=(Kfor*ky*Kcoil)/(mm*kp);
b3=Kuser/mm;

% Define continuous time system
A=[0 0 1 0;
   0 0 0 1;
   a2 0 a1 0;
   a6 a4 a5 a3;];
B=[0 0;0 0;b1 0;b2 b3];
C=[1 0 0 0];
D=0;
sysc=ss(A,B,C,D);

% Discretize system
sysd=c2d(sysc,T);
```

```
[G H C D]=ssdata(sysd);

% Partition into measurable and immeasurable state equations
Gaa=G(1:2,1:2);
Gab=G(1:2,3:4);
Gba=G(3:4,1:2);
Gbb=G(3:4,3:4);
Ha1=H(1:2,1);
Hb1=H(3:4,1);
Ha2=H(1:2,2);
Hb2=H(3:4,2);

% Place poles for deadbeat observer
L=place(Gbb,Gab,[0 0]);

% Define observer submatrices
Gr=Gbb-L*Gab;
Hy=Gr*L+Gba-L*Gaa;
Hu1=Hb1-L*Ha1;
Hu2=Hb2-L*Ha2;

% Define Integral of Error state
E=[-1 Kscale];

% Define system matrices w/o feedback control
Go=[Gaa Gab zeros(2,3);
   Gba Gbb zeros(2,3);
   Hy zeros(2) Gr [0 0]';
   E zeros(1,4) 1;];
H1=[Ha1;Hb1;Hu1;0];
H=[Ha2;Hb2;Hu2;0];

% Define PID Controller
Kc=[KP*E+KV*E*L 0 0 KV*E KI];



% Define closed-loop discrete-time system
C=[1 zeros(1,6);
   0 1 zeros(1,5);
   Kc;
   L(1,1) L(1,2) 0 0 1 0 0;
   zeros(1,6) 1;
   E zeros(1,5);];
Gcl=Go+H1*Kc;
sysd=ss(Gcl,H,C,0,T);
pole(sysd)

% =====Simulate step response=====
ydes=ones(1,length(t));
[y ts]=lsim(sysd,ydes,t);

% Assemble output
ye=y(:,1);
ym=y(:,2);
Vcoil=y(:,3);
yehd=y(:,4);
sigma=y(:,5);
err=y(:,6);
pc=(Ac/kp)*yehd-(ky*Kcoil/kp)*Vcoil;

% Plot results
figure
subplot(2,1,1)
stairs(t,err)
```

```
title('Position Error')
ylabel('error [m]')
grid on

subplot(2,1,2)
stairs(t,sigma)
title('Integrated Error')
ylabel('\sigma [m*s]')
grid on

figure
subplot(4,1,1)
stairs(t,ye,'r')
title('Bucket Position')
ylabel('Position [m]')
grid on

subplot(4,1,2)
stairs(t,ym,'b')
title('Master Position')
ylabel('Position [m]')
grid on

subplot(4,1,3)
stairs(t,Vcoil,'g')
title('Voltage to coil')
ylabel('V_c_o_i_l [V]')
grid on

subplot(4,1,4)
stairs(t,pc,'m')
title('Cylinder pressure')
ylabel('p_c [Pa]')
grid on
xlabel('kT [sec]')
```